

H₂S contributes to the hepatic arterial buffer response
and mediates vasorelaxation of the hepatic artery via
activation of K_{ATP} channels

Nikolai Siebert, Daniel Cantré, Christian Eipel, Brigitte Vollmar

Institute for Experimental Surgery, University of Rostock, 18057 Rostock, Germany

Running head: Hydrogen sulfide and hepatic arterial buffer response

Address for correspondence

Brigitte Vollmar, MD
Institute for Experimental Surgery
University of Rostock
Schillingallee 69a
D-18057 Rostock
Germany

phone: +49-381-494-6220
fax: +49-381-494-6222
e-mail: brigitte.vollmar@med.uni-rostock.de

ABSTRACT

Hepatic blood supply is uniquely regulated by the hepatic arterial buffer response (HABR), counteracting alterations of portal venous blood flow by flow changes of the hepatic artery. Hydrogen sulfide (H₂S) has been recognized as a novel signaling molecule with vasoactive properties. However, the contribution of H₂S in mediating the HABR is not studied yet. In pentobarbital-anesthetized and laparotomized rats, flow probes around the portal vein and hepatic artery allowed for assessment of the portal venous (PVBF) and hepatic arterial blood flow (HABF) under baseline conditions and stepwise reduction of PVBF for induction of HABR. Animals received either the H₂S donor Na₂S, DL-propargylglycine as inhibitor of the H₂S synthesizing enzyme cystathionine- γ -lyase (CSE), or saline alone. Additionally, animals were treated with Na₂S and the K_{ATP} channel inhibitor glibenclamide or with glibenclamide alone. Na₂S markedly increased the buffer capacity to $27.4 \pm 3.0\%$ ($P < 0.05$ vs controls: $15.5 \pm 1.7\%$), while blockade of H₂S formation by DL-propargylglycine significantly reduced the buffer capacity ($8.5 \pm 1.4\%$). Glibenclamide completely reversed the H₂S-induced increase of buffer capacity to the control level. By means of RT-PCR, Western blot analysis and immunohistochemistry, we observed the expression of both H₂S synthesizing enzymes (CSE and cystathionine- β -synthase (CBS)) in aorta, V. cava, hepatic artery and portal vein as well as in hepatic parenchymal tissue. Terminal branches of the hepatic afferent vessels expressed only CSE. We show for the first time that CSE-derived H₂S contributes to HABR and partly mediates vasorelaxation of the hepatic artery via activation of K_{ATP} channels.

Keywords: buffer capacity; DL-propargylglycine; gaseous molecules; glibenclamide; ultrasonic flowmetry

PERFUSION of the liver is unique due to its dual blood supply via the portal vein (PV) and the hepatic artery (HA). While the PV contributes to 70-80%, the HA covers about 20-30% of the total hepatic blood flow (6). Almost three decades ago, Lautt and colleagues described an intimate relationship between PV and HA, the so-called hepatic arterial buffer response (HABR), which comprises the ability of the HA to produce reciprocal compensatory flow changes in response to changes of PV flow (14). This regulatory mechanism serves not only to fulfill oxygen and metabolic demands of the liver (17, 27), but also to control overall metabolic well-being of the organism by maintaining the hepatic clearance and excretory function (11, 12).

HABR is specific to the unique vascular bed of the liver and is apparently regulated by adenosine (5, 10, 13, 16, 27). Adenosine is thought to be secreted at a constant rate into the fluid space of Mall and the concentration of adenosine is regulated by washout into the portal venules. In case of reduced PV flow, the washout of adenosine is reduced and accumulation of adenosine causes dilation of the HA, thus buffering the PV flow change (13). Beside adenosine, regulation of the hepatic vascular resistance has been shown to further involve the gaseous inorganic compounds nitric oxide (NO) and carbon monoxide (CO). While NO serves as a potent vasodilator in the HA circulation and exerts only a minor vasodilatory effect in the PV vascular bed, CO acts to maintain PV vascular tone in a relaxed state and exerts no vasodilation in the HA (24). Recently, a third gaseous mediator, hydrogen sulfide (H₂S), has been recognized as an important endogenous vasodilator and neuromodulator (32). H₂S is synthesized through degradation of cysteine by cystathionine- γ -lyase (CSE) or cystathionine- β -synthase (CBS) (7, 15, 18, 20, 29, 31). Both enzymes were found to be expressed in many mammalian tissues, including the liver (31). In the vascular system, however, CSE is suggested to be the only H₂S generating enzyme (8, 30). Hereby, vasorelaxation by H₂S is shown to be mediated by ATP-sensitive potassium channels (K_{ATP}), as effects of H₂S are mimicked by K_{ATP} openers and abolished by their inhibitors such as glibenclamide (31-33).

With respect to these vasodilatory properties of H₂S, it was the purpose of the present study to examine whether H₂S contributes to the mediation of HABR. Therefore, buffer capacity was studied in a rat model upon both exogenous application of H₂S and inhibition of the H₂S producing enzyme CSE. Furthermore, blockade of K_{ATP} channels by glibenclamide served to unravel the possible mode of action of H₂S. Moreover, the expression of the H₂S synthesizing enzymes CSE and CBS was analyzed in vascular and liver tissues.

MATERIALS AND METHODS

Materials. All drugs used in the present study were purchased from Sigma (Deisenhofen, Germany), if not stated different.

Anesthesia and monitoring. Upon approval by the local animal committee, the experiments were conducted in accordance with the German legislation on protection of animals and the NIH Guide for the Care and Use of Laboratory Animals [DHEW Publication No. (NIH) 86-23, Revised 1985]. Male Wistar rats (body weight (bw) 250-400 g; Charles River Laboratories, Sulzfeld, Germany) were used for the experiments. Animals were housed in standard animal laboratories with a 12-h light-dark cycle and had free access to water and standard laboratory chow *ad libitum*. Anesthesia was induced by intraperitoneal (ip) injection of sodium pentobarbital (50 mg x kg⁻¹ bw). Supplemental doses (25 mg x kg⁻¹ bw ip) were given during the experiment if requested to maintain sufficient anesthetic depth, which was determined by the absence of changes in blood pressure and heart rate on intermittent tail clamp. Anesthetized animals were placed in supine position on a heating pad for maintenance of body temperature (36-37°C) and were tracheotomized to facilitate spontaneous respiration (room air). Polyethylene catheters (PE 50, ID 0.58 mm; Portex, Hythe, UK) were inserted into the right carotid artery and jugular vein for assessment of central hemodynamics, blood sampling and intravenous (iv) application of drugs. Throughout the experiments, mean arterial blood pressure (MAP) and heart rate (HR) were continuously monitored.

Surgical preparation. After laparotomy, microsurgical preparation for assessment of liver blood flow was performed. In brief, ultrasonic flow probes were placed around the hepatic artery (0.5V; Transonic Systems, Ithaca, NY, USA) and the portal vein (1.5R; Transonic Systems) and were connected to a flowmeter (T402 Animal Research Flowmeter, Transonic Systems) for continuous monitoring of HA and PV blood flow values. A tourniquet loop was placed around the superior mesenteric artery (SMA) for reduction of blood flow using a micromanipulator-controlled constrictor. For assessment of hepatic tissue oxygenation, a flexible polyethylene microcatheter Clark type pO_2 probe (diameter 470 μm ; length, 300 mm) (LICOX System; GMS, Kiel-Melkendorf, Germany) was placed between the surface of two adjacent liver lobes and fixed with histoacryl glue (B. Braun, Melsungen, Germany). This allowed the probe to integrate local tissue pO_2 values over the tissue area in contact with the 5-mm long pO_2 -sensitive area near the catheter tip without interference of ambient air. Online temperature compensation was performed by an additional temperature probe (type K thermocouple probe, LICOX System), which was also positioned and fixed between two adjacent lobes. When all surgical procedures were completed, the intestine was covered with moist cloths to minimize heat loss and drying and the animals were allowed to recover from surgical stress for 30 min.

Experimental groups and protocol. The animals were allocated to the following five experimental groups ($n=10$ each): one group of animals received a continuous infusion of sodium sulfide (Na_2S , $150 \mu\text{mol} \times \text{kg}^{-1} \times \text{h}^{-1}$ iv) as donor of H_2S . For inhibition of the H_2S synthesizing enzyme CSE, animals of the second group received DL-propargylglycine (PAG, $100 \text{ mg} \times \text{kg}^{-1}$ iv) as single bolus injection, followed by a continuous infusion of isotonic saline ($3.1 \text{ ml} \times \text{h}^{-1}$ iv). For the blockade of K_{ATP} channels, animals of the third and fourth group received glibenclamide (K_{ATP} channel inhibitor) ($40 \text{ mg} \times \text{kg}^{-1}$ ip) followed by a continuous infusion either of sodium sulfide (GLB + Na_2S) or of isotonic saline (GLB) respectively. Animals which received equivalent volumes of isotonic saline only served as controls (control).

Hepatic hemodynamics, including the hepatic arterial blood flow (HABF) and portal venous blood flow (PVBF) as well as the hepatic tissue pO_2 were assessed at the following steps: (i) prior to drug application (pre), (ii) 30 min after drug application immediately before SMA tourniquet (post), and (iii) upon maximal reduction of the PVBF by complete tourniquet of the SMA, i.e. the time point at which the buffer response was quantified (SMA occlusion). The reduction of PVBF was kept constant over a time period of about 10 min followed by data assessment. In some experiments, reduction of PVBF for induction of HABR was repeated twice, allowing sufficient recovery times (~15 min) between the individual measurements for regaining baseline conditions. Arterial blood samples for blood gas analysis were taken at all time points described above. At the end of the experiment animals were killed with an overdose of iv anesthesia.

Quantification of the HABR and HA conductance. In addition to the assessment of HABF and PVBF as absolute values ($ml \times min^{-1}$), we calculated the total hepatic blood flow (THBF) as the sum of HABF and PVBF. Further, we determined the buffer capacity as change of HABF divided by the change of PVBF $\times 100$ (26) as well as the HA conductance calculated as HABF per kilogram of body weight divided by MAP ($ml \times min^{-1} \times kg^{-1} \times mmHg^{-1}$) (22).

RT-PCR. Total RNA was isolated from liver and vascular tissues using a RNeasy Mini Kit (Qiagen, Germany) according to the manufacturer's instructions. RNA concentration was determined spectrophotometrically. First strand cDNA was synthesized by reverse transcription of 2 μg of total RNA using oligo(dT)18 primer (Biolabs, Frankfurt am Main, Germany) and Superscript II RNaseH-Reverse Transcriptase (Invitrogen, Karlsruhe, Germany) in the presence of dNTP's, 5 x first strand buffer and dithiothreitol at 72°C for 10 min and 42°C for 60 min. The reverse transcriptase was inactivated by 95°C for 5 min. Rat CSE and CBS were amplified by 24 cycles of PCR consisting of 94°C (30s) for denaturation, 58°C (CSE) or 56°C (CBS) (30s) for primer-specific annealing and 72°C (30s) for extension using Taq polymerase (Amersham Bioscience, Piscataway, NJ, USA). For the detection of CSE mRNA, the forward primer sequence used was 5'-CAT GGA TGA AGT GTA TGG AGG

C-3', and the reverse primer sequence was 5'-CGA TTG TTA CCT CTG CTG CCG-3'. The PCR product size was 445 bp. For the detection of CBS mRNA, the forward primer sequence used was 5'-GAT GAC ACC GCA GAG GAG AT-3', and the reverse primer sequence was 5'-CGG GAT CTA CAC CGA TGA TT-3'. The PCR product size was 150 bp. The reaction without RNA template (none template control (NTC)) was also performed as a negative control. In a comparable assay, the RNA integrity and cDNA synthesis was tested using rat GAPDH as a housekeeping gene and the following primers: 5'-AAC GAC CCC TTC ATT GAC-3' and 5'-TCC ACG ACA TAC TCA GCA C-3'. PCR products were separated by electrophoresis on 2.0% agarose gels. Ethidium-bromide-stained bands were visualized by UV illumination and densitometrically semi-quantified (TotalLab, Nonlinear Dynamics, New Castle upon Tyne, UK). The data represent expression of CSE and CBS gene product in relation to that of GAPDH.

Western blot analysis. For Western blot analysis of CSE and CBS, liver tissue was homogenized in lysis buffer (1 M Tris pH 7.5, 5 M NaCl, 250 mM EDTA, 10% Triton-X 100, 4% NaN₃, and 100 mM PMSF), incubated for 30 min on ice, and centrifuged for 15 min at 10000 x g. Prior to use, all buffers received a protease inhibitor cocktail (1:100 vol/vol; Sigma). Protein concentrations were determined using the BCA protein assay (Pierce, Rockford, IL, USA) with bovine serum albumin as standard. Equal amounts of whole protein extracts (20 µg) were separated discontinuously on sodium dodecyl sulphate polyacrylamide gels (12% SDS-PAGE) and transferred to a polyvinylidene difluoride membrane (Immobilon-P transfer membrane; Millipore, Billerica, MA, USA). After blockade of non-specific binding sites, membranes were incubated for 2 h at room temperature with mouse monoclonal anti-CSE (1:1000; ABNOVA Corporation, Taipei, Taiwan) or goat polyclonal anti-CBS (1:2000; Santa Cruz Biotechnology, Inc., Europe), followed by peroxidase-conjugated goat anti-mouse IgG antibody for CSE (1:2000; LSAB+Systems-HRP; Dako, Germany) and donkey anti-goat IgG antibody for CBS (1:5000; Santa Cruz Biotechnology Inc., Europe) as secondary antibodies. Protein expression was visualized by means of luminol enhanced chemiluminescence (ECL plus; Amersham Pharmacia Biotech, Freiburg, Germany) and

exposure of the membrane to a blue light sensitive autoradiography film (Kodak BioMax Light Film, Kodak-Industrie, Chalon-sur-Saone, France). Signals were densitometrically assessed (TotalLab) and normalized to the β -actin signals (monoclonal mouse anti- β -actin antibody, 1:20000; Sigma Aldrich, Saint Louis, USA) followed by peroxidase-conjugated rabbit anti-mouse IgG antibody for β -actin (1:60000; Sigma Aldrich, Saint Louis, USA).

Immunohistochemistry. Liver and vascular tissue (portal vein, hepatic artery, aorta and V. cava) was fixed in 4% phosphate buffered formalin for 2–3 days and embedded in paraffin. For immunohistochemical demonstration of CSE and CBS, sections collected on poly-L-lysine-coated glass slides were treated by microwave for antigen unmasking. Mouse monoclonal anti-CSE antibody (1:500; ABNOVA Corporation) and goat polyclonal anti-CBS antibody (1:100; Santa Cruz Biotechnology Inc., Europe) were used as primary antibodies and incubated for 18 h at 4°C. After equilibrating to room temperature, sections were incubated with horseradish peroxidase-conjugated secondary antibodies (LSAB+Systems-HRP; Dako, Germany). 3-amino-9-ethylcarbazole was used as chromogen (Dako, Germany). Then the sections were counterstained with hemalaun and examined by light microscopy (Axioskop 40, Zeiss, Göttingen, Germany).

Statistical analysis. After testing for normality and equal variance across groups, differences between groups were assessed using one-way ANOVA test. A *P* level of <0.05 was considered significant. All data are given as means \pm standard error of the mean (SEM). Analysis was performed using the software package SigmaStat (Jandel, San Rafael, CA, USA).

RESULTS

Infusion of Na₂S resulted in a transient (~ 60 sec) decrease of MAP indicative for the vasoactive property of H₂S (Fig. 1A). Astonishingly, MAP regained baseline values at latest after 2 min (Fig. 1A), although Na₂S was infused continuously. All other drugs did not even transiently affect systemic hemodynamics (Table 1). Animals exhibited no signs of transient awareness due to insufficient anesthetic depth as assessed by negative tail clamp testing or

lack of withdrawal of paw pinch. Blood gas analysis revealed no significant differences with an arterial pO_2 of 95.5 ± 1.0 mmHg, pCO_2 of 50.4 ± 0.5 mmHg and pH values of 7.37 ± 0.01 among the groups studied.

The application of the respective drugs did not significantly influence the PVBF and the HABF compared with the respective values of the control animals (Fig. 2). However, it is important to mention that the initial Na_2S -induced drop in blood pressure was paralleled by a transient decrease in HABF, which was followed by a transient elevation of blood flow, representing hepatic arterial vasodilation (Fig. 1C).

As expected, the reduction of PVBF initiated a pronounced HABR, indicated by a significant increase of HABF in all groups studied. The degree of PV flow reduction did not differ between the individual animals or between the groups and approximated 70% of the baseline values (Fig. 2, A-E). The maximal increase of HA inflow could be observed in the Na_2S group (Fig. 2G), while the least pronounced HA increase occurred upon the inhibition of H_2S producing enzyme by PAG (Fig. 2H).

Analyzing the buffer capacity, livers of the Na_2S -treated animals exhibited the maximal compensation among the groups (Fig. 3A). The lowest buffer capacity was observed in animals, which received the CSE inhibitor PAG. Glibenclamide administration reversed the Na_2S -induced increase of buffer capacity to the level found in the control group, and glibenclamide alone did not influence buffer capacity at all. Calculating the HA conductance, highest values were found after the application of Na_2S , while PAG administration presented with lowest HA conductance (Fig. 3B). The pretreatment with glibenclamide followed by Na_2S infusion resulted in reduction of the HA conduction to the level of the control group (Fig. 3B). The hepatic tissue oxygenation was found comparable in all five groups of animals during both baseline conditions and after the drug supplementation (22.2 ± 0.7 mmHg), but decreased upon maximal reduction of PV blood flow without significant differences between groups (16.1 ± 0.6 mmHg).

As illustrated in Fig. 4 and Fig. 5, mRNAs encoding for CSE and CBS were expressed in rat liver tissue. Protein of CSE and CBS could also be detected in liver tissue. The

application of the respective drugs did change the basal expression of these two H₂S synthesizing enzymes at neither mRNA- nor protein level (Figs. 4 and 5). In addition, the mRNAs encoding for both enzymes were also detected in the vascular system, including the hepatic artery, portal vein, aorta and V. cava (Fig. 6, A and E). In line with this, immunohistochemistry of PV and HA (Fig. 6, B and F) as well as of aorta and V. cava (Fig. 6, C and G) revealed positive staining for CSE and CBS. In addition, strong immunoreactivity for CSE and CBS could be observed in hepatic parenchymal tissue (Fig 6, D and H). Of interest, terminal branches of the HA and PV within the portal triads were found positive for CSE (Fig. 6D), but not for CBS (Fig. 6H).

DISCUSSION

In the present study we provide major evidence that H₂S contributes to the HABR and partly mediates the vasodilative response of the HA. This conclusion is based on the fact that the supplementation of H₂S increased HA conductance and almost doubled the buffer capacity. Vice-versa inhibition of the H₂S synthesis markedly decreased buffer capacity. Furthermore, we could show that vasorelaxation of HA by H₂S was inhibited by application of a selective inhibitor of K_{ATP} channels. The two H₂S synthesizing enzymes CSE and CBS were found expressed in vessels of the systemic and hepatic circulation. Intrahepatic terminal branches of the HA and PV however lack CBS, but not CSE expression.

Methodological considerations. The magnitude or efficacy of the buffer response varies depending on the technique employed and on the condition of the animal (11, 14). In contrast to previous reports of other groups we placed the ultrasonic flow probes directly around the HA and the PV without ligation of the splenic artery, the left gastric artery, the gastroduodenal artery and inlet arteries to the splanchnic system (10, 21, 26). In our case, the maximal SMA occlusion did not cause zero flow of PVBF and thus did not provoke maximal HABR. However, the methodology used here is less traumatic and does not require the ligation of arteries supplying the upper splanchnic area with the positive consequence that buffer response is not pre-activated, as this has been described by our group in a

previous study upon ligation of the arteries mentioned above (27). Data of the total hepatic blood flow are in good accordance with the results of previously published studies (3, 25-27), underlining the reliability of the present methodological approach.

Mathie et al. postulated that PV provides the major blood supply of oxygen to the liver and that its loss could lead to a certain degree of hepatic hypoxia (16). In line with the present observation that HABR could not fully compensate for reduced PV inflow, hepatic tissue oxygenation was found reduced during SMA occlusion, but still in the physiological range of liver tissue pO_2 (21, 27). At first sight, these findings contrast previous data of our group, demonstrating that upon reduction of PVBF hepatic tissue oxygenation was maintained (21, 27). This discrepancy might be due to the different methodologies and surgical approaches, used in the present study for induction of HABR. The current technique with HA dissection and direct placement of the ultrasonic flow probe might have increased vascular tone, which would further explain the less pronounced buffer capacity compared to the respective values of one of our previous studies (26).

The used H_2S donor Na_2S is an easy and fast soluble substance, which dissociates to Na^+ and S^{2-} ; the latter then binds H^+ to form HS^- as well as H_2S . To inhibit endogenous production of H_2S , PAG was used as an inhibitor of CSE. Though PAG and β -cyanoalanine (BCA) are well known CSE inhibitors (19), we preferred to use PAG. It has been reported that the reversible inhibitor BCA is less effective than the irreversible inhibitor PAG in that livers from BCA pre-treated animals exhibited less inhibition of H_2S formation than livers from PAG pre-treated animals (19). Noteworthy, in the present experiments, the supplementation of the respective drugs did not influence basal PVBF, HABF or systemic hemodynamic parameters. Thus, it is reasonable to state that the observed changes upon PV flow reduction are exclusively due to the local, i.e. hepatic action of the drugs.

HABR and H_2S . It has been shown that H_2S relaxed rat thoracic aorta, portal vein and mesenteric arteries *in vitro* (4). Moreover, an intravenous bolus injection of H_2S decreased dose-dependently MAP in anesthetized rats (33). In line with our present data this H_2S -induced vasodilative effect was transient in nature (33). Zhao et al. further reported on a

direct effect of H₂S on vascular smooth muscle cells, thereby mediating vasodilatation (33). However, the mechanism of H₂S action is not fully understood. The ability of H₂S to relax vascular smooth muscle cells most likely occurs through activation of ATP-sensitive K⁺ channels (31). K_{ATP} channels are present in almost all tissues, including vascular smooth muscle. The change in potassium conductance of the smooth muscle cell membrane produces a relaxation of blood vessels (9, 23, 28). To elucidate whether K_{ATP} channels were the target of H₂S in the hepatic artery, glibenclamide was administered. H₂S-induced relaxation of the HA was found abolished by glibenclamide, which confirms the notion that K_{ATP} channels in vascular smooth muscle cells are the target of H₂S (33).

Preliminary experiments of our group with application of the adenosine receptor-1 antagonist 8-theophylline for blockage of HABR indicated that concomitant infusion of Na₂S was capable to partly reverse the HABR blockage (data not shown). These observations imply that H₂S is working rather independent of adenosine in mediation of HABR. However, further investigations are necessary to unravel the complex interactions between H₂S, adenosine and other gaseous mediators in the context of regulation of liver blood supply.

It has been postulated that the mediators responsible for the HA dilation were acting upstream from the hepatic sinusoids (2). We studied the expression of H₂S synthesizing enzymes in aorta and V. cava as well as HA and PV including their intrahepatic terminal branches within the portal triads. Current data suggest that CBS is the predominant H₂S generating enzyme in brain and nervous system, whereas only CSE was identified in the vascular system, including the rat aorta and mesenteric artery (4, 8, 30). In line with this, we could find the expression of CSE in aorta and V. cava as well as in HA and PV at both mRNA- and protein level. However, we extend the current knowledge of other groups (1, 31, 33) in that we could observe the second enzyme CBS, being also expressed in the large vessels studied. In addition, we can report that intrahepatic terminal branches of the HA and PV were found positive for CSE, but not for CBS. With the assumption that the space of Mall is the potential site of the mediator-driven communication between the HA and the PV (10), it is thus reasonable to speculate that HABR-associated vasodilatation of HA is partly mediated

by H₂S, which is predominantly synthesized by CSE. There is evidence that endogenous production of H₂S depends on the vessel type. So, Zhao et al. have found about five-fold higher sensitivity of mesenteric artery beds to H₂S than of aortic tissues (33), whereas Hosoki et al. have shown that the homogenates of thoracic aortas yielded more H₂S than that of portal vein of rats (7). The mechanisms for vascular type selective sensitivities to H₂S are not fully understood and remain to be clarified. However, we provide first evidence for a differential expression of CSE and CBS in the intrahepatic vascular system.

In summary, our data strongly underscore that H₂S increases the HA buffer capacity via activation of K_{ATP} channels. In addition, H₂S seems to be released from CSE in the terminal hepatic afferent vessels.

ACKNOWLEDGEMENTS

The authors cordially thank Berit Blendow, Doris Butzlaff, Dorothea Frenz and Maren Nerowski (Institute for Experimental Surgery, University of Rostock) for excellent technical assistance. The study is supported by a grant from the Deutsche Forschungsgemeinschaft (Vo 450/7-3; Bonn, Bad Godesberg).

REFERENCES

1. **Abe K, Kimura H.** The possible role of hydrogen sulfide as an endogenous neuromodulator. *J Neurosci* 16: 1066-1071, 1996.
2. **Ayuse T, Brienza N, O'Donnell CP, Robotham JL.** Pressure-flow analysis of portal vein and hepatic artery interactions in porcine liver. *Am J Physiol* 267: H1233-H1242, 1994.
3. **Baer HU, Guastella T, Wheatley AM, Zimmermann A, Blumgart LH.** Acute effects of partial hepatectomy on liver blood flow in the jaundiced rat. *J Hepatol* 19: 377-382, 1993.
4. **Cheng Y, Ndisang JF, Tang G, Cao K, Wang R.** Hydrogen sulfide-induced relaxation of resistance mesenteric artery beds of rats. *Am J Physiol Heart Circ Physiol* 287: H2316-H2323, 2004.
5. **Ezzat WR, Lutt WW.** Hepatic arterial pressure-flow autoregulation is adenosine mediated. *Am J Physiol* 252: H836-H845, 1987.
6. **Greenway CV, Stark RD.** Hepatic vascular bed. *Physiol Rev* 51: 23-65, 1971.
7. **Hosoki R, Matsuki N, Kimura H.** The possible role of hydrogen sulfide as an endogenous smooth muscle relaxant in synergy with nitric oxide. *Biochem Biophys Res Commun* 237: 527-531, 1997.
8. **Ishii I, Akahoshi N, Yu XN, Kobayashi Y, Namekata K, Komaki G, Kimura H.** Murine cystathionine gamma-lyase: complete cDNA and genomic sequences, promoter activity, tissue distribution and developmental expression. *Biochem J* 381: 113-123, 2004.
9. **Kovacs RJ, Nelson MT.** ATP-sensitive K⁺ channels from aortic smooth muscle incorporated into planar lipid bilayers. *Am J Physiol* 261: H604-H609, 1991.
10. **Lutt WW, Legare DJ, d'Almeida MS.** Adenosine as putative regulator of hepatic arterial flow (the buffer response). *Am J Physiol* 248: H331-H338, 1985.
11. **Lutt WW, Legare DJ, Ezzat WR.** Quantitation of the hepatic arterial buffer response to graded changes in portal blood flow. *Gastroenterology* 98: 1024-1028, 1990.

12. **Lautt WW.** Mechanism and role of intrinsic regulation of hepatic arterial blood flow: hepatic arterial buffer response. *Am J Physiol* 249: G549-G556, 1985.
13. **Lautt WW.** Regulatory processes interacting to maintain hepatic blood flow constancy: Vascular compliance, hepatic arterial buffer response, hepatorenal reflex, liver regeneration, escape from vasoconstriction. *Hepatol Res* 37: 891-903, 2007.
14. **Lautt WW.** Relationship between hepatic blood flow and overall metabolism: the hepatic arterial buffer response. *Fed Proc* 42: 1662-1666, 1983.
15. **Lu Y, O'Dowd BF, Orrego H, Israel Y.** Cloning and nucleotide sequence of human liver cDNA encoding for cystathionine gamma-lyase. *Biochem Biophys Res Commun* 189: 749-58, 1992.
16. **Mathie RT, Alexander B.** The role of adenosine in the hyperaemic response of the hepatic artery to portal vein occlusion (the 'buffer response'). *Br J Pharmacol* 100: 626-630, 1990.
17. **Mathie RT, Blumgart LH.** The hepatic haemodynamic response to acute portal venous blood flow reductions in the dog. *Pflugers Arch* 399: 223-227, 1983.
18. **Meier M, Janosik M, Kery V, Kraus JP, Burkhard P.** Structure of human cystathionine beta-synthase: a unique pyridoxal 5'-phosphate-dependent heme protein. *EMBO J* 20: 3910-3916, 2001.
19. **Mok YY, Atan MS, Yoke Ping C, Zhong Jing W, Bhatia M, Moochhala S, Moore PK.** Role of hydrogen sulphide in haemorrhagic shock in the rat: protective effect of inhibitors of hydrogen sulphide biosynthesis. *Br J Pharmacol* 143: 881-889, 2004.
20. **Moore PK, Bhatia M, Moochhala S.** Hydrogen sulfide: from the smell of the past to the mediator of the future? *Trends Pharmacol Sci* 24: 609-611, 2003.
21. **Mücke I, Richter S, Menger MD, Vollmar B.** Significance of hepatic arterial responsiveness for adequate tissue oxygenation upon portal vein occlusion in cirrhotic livers. *Int J Colorectal Dis* 15: 335-341, 2000.

22. **Munding TO, Taborsky GJ Jr.** Differential action of hepatic sympathetic neuropeptides: metabolic action of galanin, vascular action of NPY. *Am J Physiol Endocrinol Metab* 278: E390-E397, 2000.
23. **Nelson MT, Quayle JM.** Physiological roles and properties of potassium channels in arterial smooth muscle. *Am J Physiol* 268: C799-C822, 1995.
24. **Pannen BH.** New insights into the regulation of hepatic blood flow after ischemia and reperfusion. *Anesth Analg* 94: 1448-1457, 2002.
25. **Prins HA, Houdijk AP, Wiezer MJ, Teerlink T, van Lambalgen AA, Thijs LG, van Leeuwen PA.** The effect of mild endotoxemia during low arginine plasma levels on organ blood flow in rats. *Crit Care Med* 28: 1991-1997, 2000.
26. **Richter S, Mücke I, Menger MD, Vollmar B.** Impact of intrinsic blood flow regulation in cirrhosis: maintenance of hepatic arterial buffer response. *Am J Physiol Gastrointest Liver Physiol* 279: G454-G462, 2000.
27. **Richter S, Vollmar B, Mücke I, Post S, Menger MD.** Hepatic arteriolo-portal venular shunting guarantees maintenance of nutritional microvascular supply in hepatic arterial buffer response of rat livers. *J Physiol* 531: 193-201, 2001.
28. **Standen NB, Quayle JM, Davies NW, Brayden JE, Huang Y, Nelson MT.** Hyperpolarizing vasodilators activate ATP-sensitive K⁺ channels in arterial smooth muscle. *Science* 245: 177-180, 1989.
29. **Stipanuk MH, Beck PW.** Characterization of the enzymic capacity for cysteine desulphhydration in liver and kidney of the rat. *Biochem J* 206: 267-77, 1982.
30. **Stipanuk MH.** Sulfur amino acid metabolism: pathways for production and removal of homocysteine and cysteine. *Annu Rev Nutr* 24: 539-577, 2004.
31. **Wang R.** Two's company, three's a crowd: can H₂S be the third endogenous gaseous transmitter? *FASEB J* 16: 1792-1798, 2002.
32. **Zhao W, Wang R.** H(2)S-induced vasorelaxation and underlying cellular and molecular mechanisms. *Am J Physiol Heart Circ Physiol* 283: H474-H480, 2002.

33. **Zhao W, Zhang J, Lu Y, Wang R.** The vasorelaxant effect of H₂S as a novel endogenous gaseous K(ATP) channel opener. *EMBO J* 20: 6008-6016, 2001.

FIGURE LEGENDS

Fig. 1. Mean arterial blood pressure (MAP; A), portal venous blood flow (PVBF; B) and hepatic arterial blood flow (HABF; C) after the administration of the H₂S donor Na₂S (arrow indicates start of infusion). Values are means ± SEM of three independent experiments.

Fig. 2. Portal venous (PVBF, A-E) and hepatic arterial (HABF, F-J) blood flow during baseline conditions (pre), after the drug supplementation (post) and upon maximal SMA occlusion. Animals received isotonic saline (control; A, F), the H₂S donor Na₂S (Na₂S; B, G), the CSE inhibitor DL-propargylglycine (PAG; C, H), the K_{ATP} channel inhibitor glibenclamide combined with Na₂S (GLB + Na₂S; D, I), or glibenclamide alone (GLB; E, J). Values are means ± SEM of ten independent experiments per group. ANOVA, followed by appropriate post hoc comparison test; * $P < 0.05$ vs. pre; # $P < 0.05$ vs. post.

Fig. 3. Buffer capacity as change of HABF divided by the change of PVBF x 100 (A) and change of hepatic arterial conductance upon maximal SMA occlusion compared to values assessed at the time point immediately before SMA occlusion (B). Animals received isotonic saline (control), the H₂S donor Na₂S (Na₂S), the CSE inhibitor DL-propargylglycine (PAG), the K_{ATP} channel inhibitor glibenclamide combined with Na₂S (GLB + Na₂S) or glibenclamide alone (GLB). Values are means ± SEM of ten independent experiments per group. ANOVA, followed by appropriate post hoc comparison test; * $P < 0.05$ vs. control; # $P < 0.05$ vs. Na₂S.

Fig. 4. Representative RT-PCR (A) and densitometric analysis (B) of CSE mRNA expression as well as Western blot (C) and densitometric analysis (D) of CSE protein expression in liver tissue. Animals received isotonic saline (control), the H₂S donor Na₂S (Na₂S), the CSE inhibitor DL-propargylglycine (PAG), the K_{ATP} channel inhibitor glibenclamide combined with Na₂S (GLB + Na₂S) or glibenclamide alone (GLB). NTC, none template control (negative control). Signals were corrected with that of GAPDH or β-actin serving as internal control for

mRNA and protein expression analysis, respectively. Values are given as means \pm SEM of ten independent experiments per group.

Fig. 5. Representative RT-PCR (A) and densitometric analysis (B) of CBS mRNA expression as well as Western blot (C) and densitometric analysis (D) of CBS protein expression in liver tissue. Animals received isotonic saline (control), the H₂S donor Na₂S (Na₂S), the CSE inhibitor DL-propargylglycine (PAG), the K_{ATP} channel inhibitor glibenclamide combined with Na₂S (GLB + Na₂S) or glibenclamide alone (GLB). NTC, none template control (negative control). Signals were corrected with that of GAPDH or β -actin serving as internal control for mRNA and protein expression analysis, respectively. Values are given as means \pm SEM of ten independent experiments per group.

Fig. 6. Representative RT-PCR analysis of CSE (A) and CBS mRNA expression (E) in vascular and liver tissue. GAPDH served as internal control. Representative immunohistochemical images of CSE (left row) and CBS expression (right row) of the hepatic artery (HA) and portal vein (PV) (B, F), aorta and vena cava (C, G) as well as liver tissue, displaying a portal triad (D, H). NTC, none template control (negative control).

TABLES

Table 1: Mean arterial blood pressure (MAP) and heart rate (HR) during baseline conditions (pre), 30 min after drug supplementation (post) and upon maximal SMA occlusion. Animals received isotonic saline (control), the H₂S donor Na₂S (Na₂S), the CSE inhibitor DL-propargylglycine (PAG), the K_{ATP} channel inhibitor glibenclamide combined with Na₂S (GLB + Na₂S) or glibenclamide alone (GLB).

parameter	groups	pre	post	SMA occlusion
MAP, mmHg	control	114 ± 4	115 ± 5	120 ± 5
	Na ₂ S	116 ± 3	120 ± 5	127 ± 5
	PAG	109 ± 4	118 ± 3	120 ± 3
	GLB + Na ₂ S	115 ± 4	113 ± 3	118 ± 3
	GLB	118 ± 3	116 ± 2	126 ± 2
	HR, min ⁻¹	control	368 ± 12	364 ± 11
Na ₂ S		387 ± 9	369 ± 9	369 ± 13
PAG		384 ± 13	400 ± 14	392 ± 13
GLB + Na ₂ S		327 ± 6	318 ± 7	316 ± 7
GLB		339 ± 6	329 ± 6	326 ± 7

Values are given as means ± SEM of ten independent experiments per group.

Figure 1

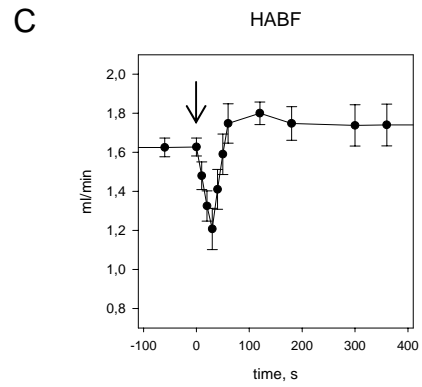
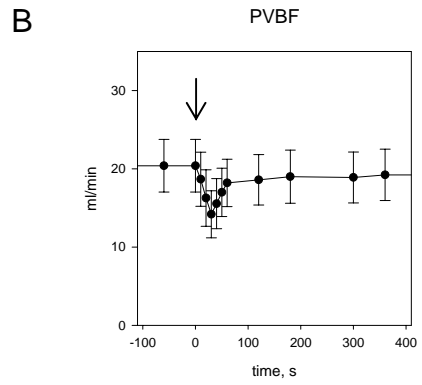
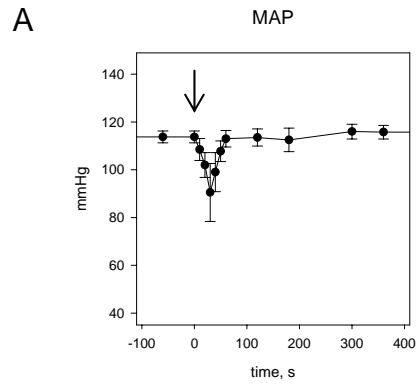


Figure 2

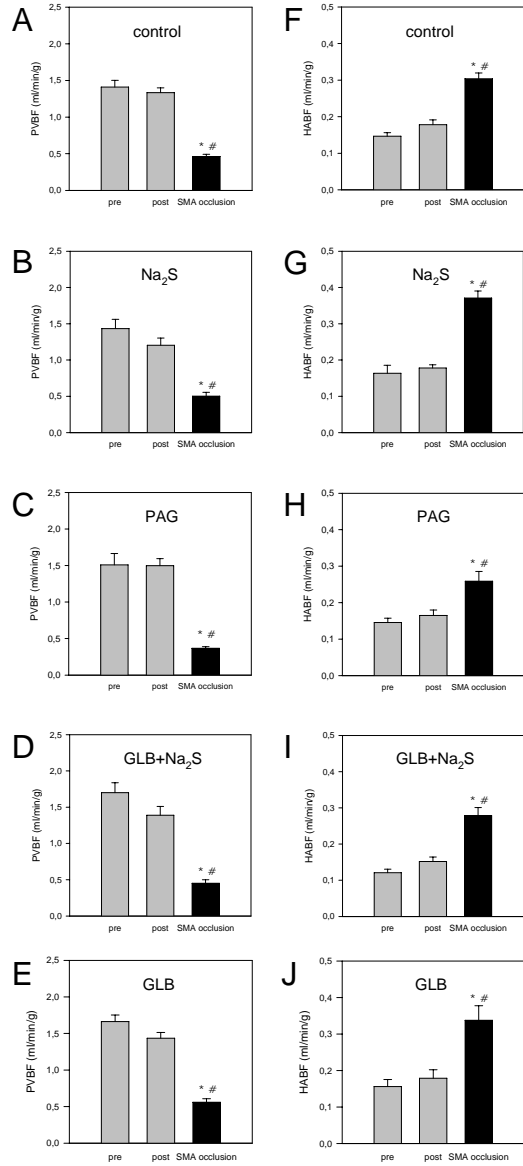


Figure 3

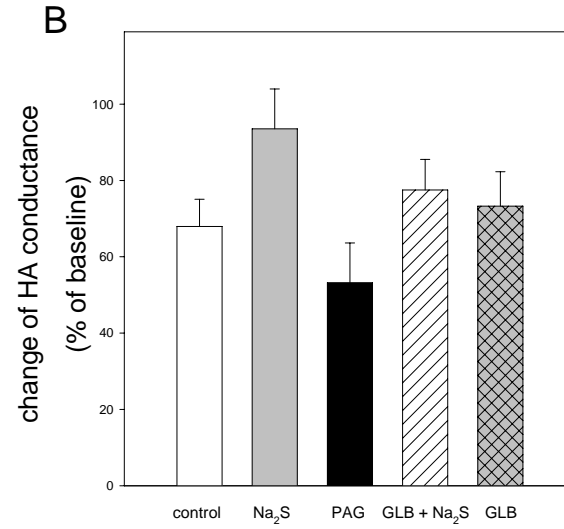
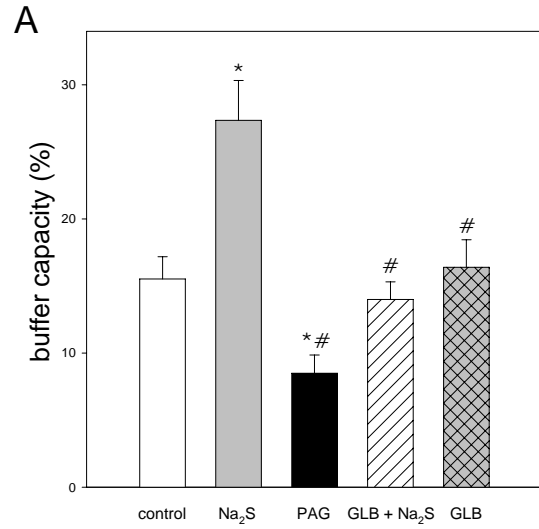


Figure 4

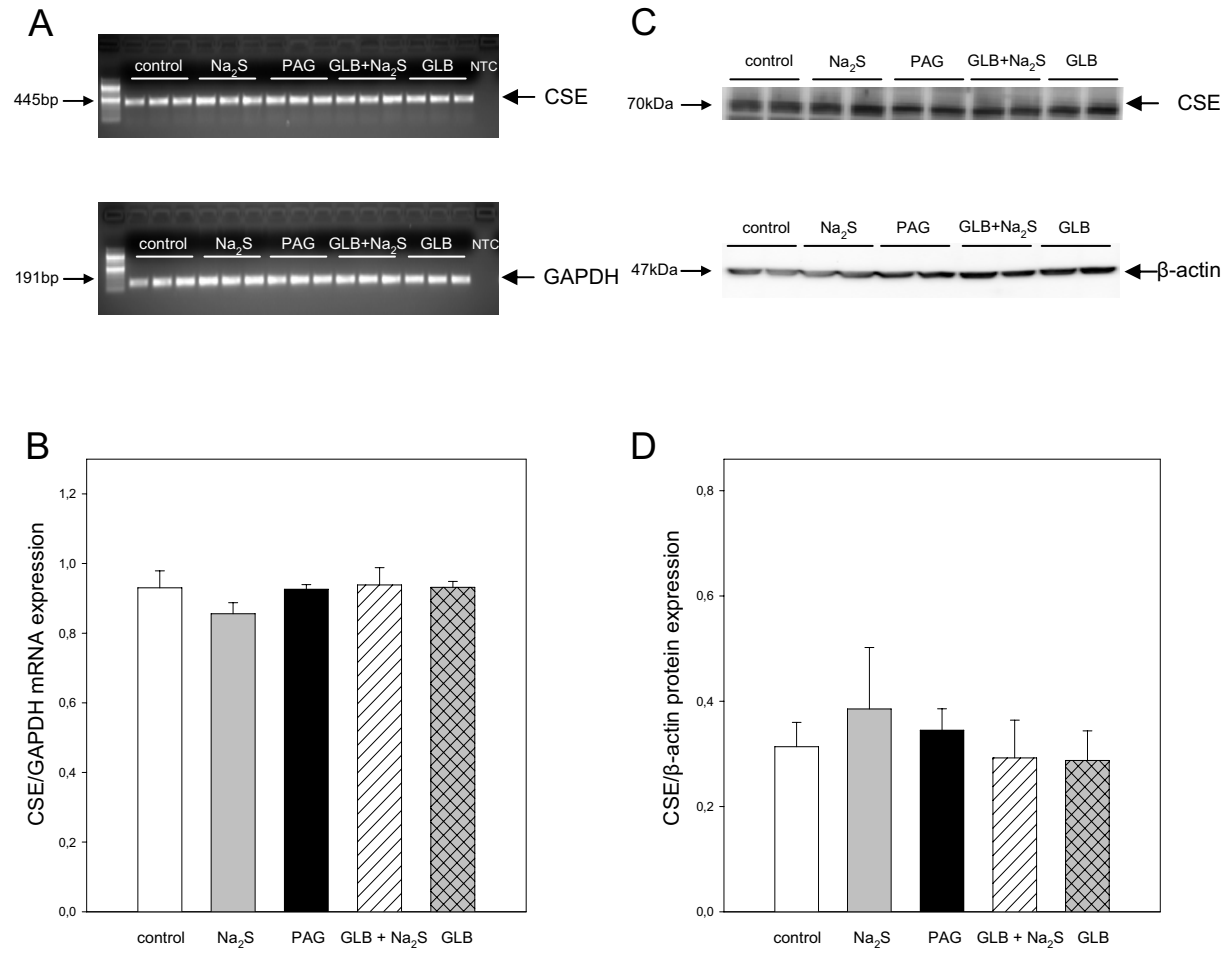


Figure 5

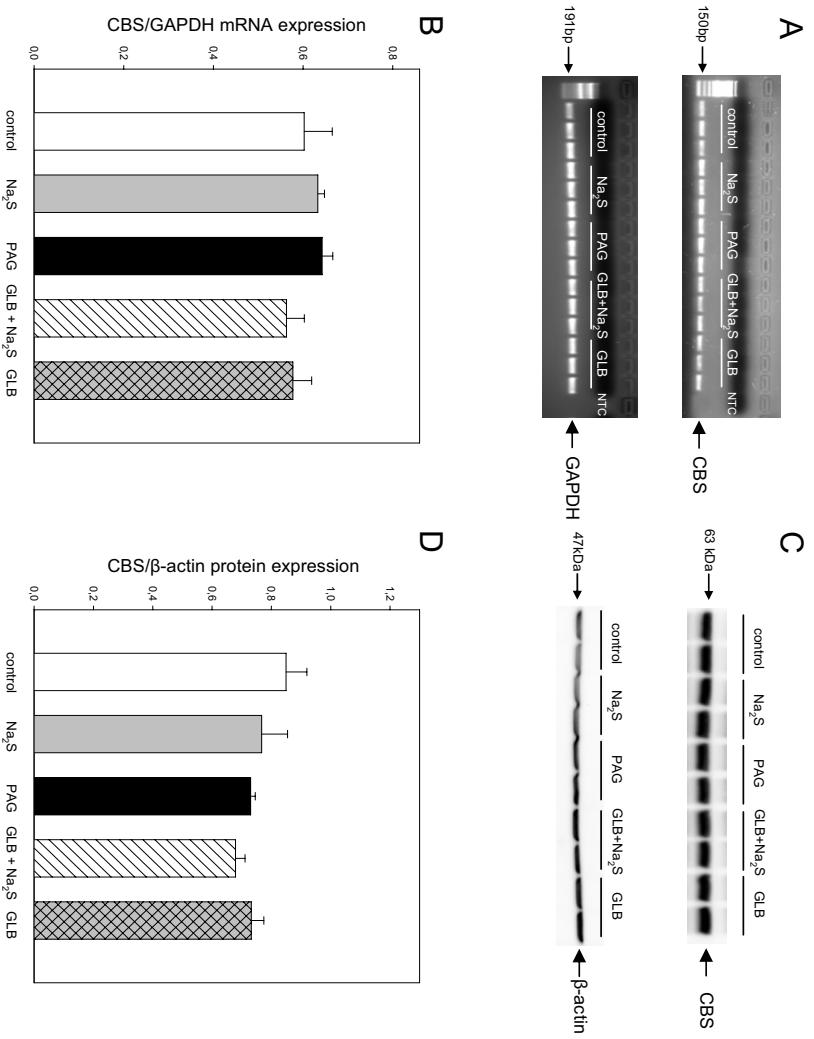


Figure 6

